ELSEVIER

Sensors and Actuators A 99 (2002) 277–283

SENSORS AND ACTUATORS A PHYSICAL

www.elsevier.com/locate/sna

LiCAF crystal-based optical fiber thermometry

M. Stanciu[a], K.T.V. Grattan[b,*]

[a]*Universite Polytechnique de Bucarest, Splaiul Independentei 313, 77206 Bucarest, Romania*

[b]*Department of Electrical, Electronic & Information Engineering, City University, Northampton Square, London EC1V 0HB, UK*

Received 4 August 2000; received in revised form 11 April 2001; accepted 22 April 2001

Abstract

Experiments are reported on a LiCAF crystal-based optical fiber thermometer, and results given for the performance over the region from 300 to 550 K for two crystal samples, of different doping levels. The system is simple to implement and offers good measurement potential over this important temperature region.

Keywords: Thermometer; Crystal; Fiber optic; Fluorescence

1. Introduction

A wide range of techniques for optical fiber thermometry has been reported and, amongst these the use of doped fibers in silica and polymer materials, bulk glasses and crystals have shown considerable promise [1]. The limitations of the incorporation of doped fibers are being seen in some recent work, due to the long term stability of the material [2] and the use of crystalline fibers, whilst promising, shows the weakness of the production method in its failure to achieve long, flexible clad fibers. The incorporation of appropriate crystal probe materials in sensor systems has been successful in the past [1] and still continues to offer new opportunities for specific sensing needs. The rapid growth in the use of crystalline materials for laser applications enhances the choices from those available to the sensor designer and reflects the potential to create new and effective sensor probes.

In this paper, further work on the use of chromium (Cr^{3+}) doped crystals is presented. Ruby, the most common (Cr^{3+} in sapphire) has its limitations [1] and other Cr^{3+} doped materials can offer advantages, as is discussed in this paper. This is highly compatible with the use of the approach based on monitoring the fluorescence decay time, the reduction in which is monitored as a measure of temperature rise and whose advantages are described elsewhere [1].

Thus, for these temperature sensors, it is preferable to use crystals with the absorption and fluorescence spectra in the visible or near infrared domain, especially at and beyond the red part of the spectrum, rather than in the ultraviolet where often strong absorption is seen because in this case, the usual and inexpensive electrooptical components (ultrabright LEDs or laser diodes and pin photodiodes or pin-FET modules) can be used. Also, these components have other important advantages including small dimensions, a good coupling to optical fibers and a long operational lifetime.

To complement this, the selection of the most appropriate choice of fluorescent crystal must take into account the best of the technological aspects, such as the physical characteristics (durability, thermal conductivity and robustness) of the sensor components, i.e. the optical fibers, the ceramic inserts, the muffs and the adhesives.

2. Theoretical background

In the ionic lattices, the Cr^{3+} ions have a strong interaction both with the field strength of the host crystal and with the lattice vibrations. As a result, crystals activated with Cr^{3+} ions have a broad optical absorption spectrum, from the ultraviolet to infrared domain of the visible spectrum. Also, on account of this strong crystal field interaction, the energy gaps of the electronic levels of Cr^{3+} depend on the host crystal type, this being the phenomenon that generates the different temperature dependences of the fluorescence lifetime of Cr^{3+} doped crystals [1].

The electronic energy levels of the Cr^{3+} ions are illustrated in the simplified Tanabe–Sugano diagram [3] (Fig. 1), which plots the normalized energy of the low lying excited states (E/B) as a function of the normalized octahedral

* Corresponding author. Tel.: +44-207-040-8120; fax: +44-207-040-8121.
E-mail address: k.t.v.grattan@city.ac.uk (K.T.V. Grattan).

0924-4247/02/$ – see front matter
PII: S0924-4247(01)00795-6

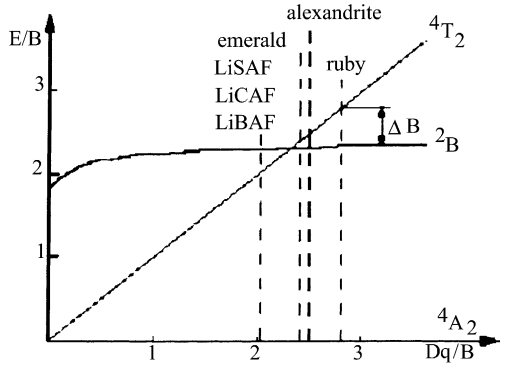

Fig. 1. Simplified Tanabe–Sugano diagram.

crystal field strength (Dq/B) for various host crystals: ruby (Cr^{3+}:$A1_2O_3$), emerald, alexandrite, LiBAF (Cr^{3+}:LiBaAlF$_6$), LiSAF (Cr^{3+}:LiSrAlF$_6$), and LiCAF (Cr^{3+}:LiCaAlF$_6$), the last of these being the subject for this study. The ground state is always the orbital singlet ($^4A_2$). The diagram also shows the energy level position of the Cr^{3+} ion in various host crystals. The energy splitting (ΔE) between the low lying state ($^4T_2$) and the state ^2E is defined by:

$$\Delta E = E(^4T_2) - E(^2E) \quad (1)$$

In a high strength crystal field, $Dq/B \gg 2.3$ (as in case of the ruby [4] emerald and alexandrite), $\Delta E > 0$, and the fluorescent emission is dominated by the sharp R lines ($^2E \rightarrow {}^4A_2$ transition), for example, ruby has $\Delta E \cong 2350\ cm^{-1}$.

In a low strength crystal field, $Dq/B \ll 2.3$ (as in case of the LiSAF, LiCAF and LiBAF), $\Delta E < 0$, the fluorescent emission is dominated by the broad $^4T_2 \rightarrow {}^4A_2$ band transition.

The intrinsic lifetime of the Cr^{3+} ions of the $^4T_2$ state is much shorter than that of the $^4A_2$ state and so the magnitude of Dq/B gives the temperature dependence of the Cr^{3+} fluorescence lifetimes, revealing their different characteristics.

In a *high field crystal*, at low temperatures, the Cr^{3+} fluorescence is dominated by $^2E \rightarrow {}^2A_4$ transitions. Thus, for these transitions, long fluorescence lifetimes are observed, e.g. ≅3.5 ms at 300 K, familiar for ruby. At high temperatures, a higher percentage of the excited Cr^{3+} ions will populate the short lifetime $^4T_2$ state and consequently more $^4T_2 \rightarrow {}^2A_4$ transitions will be initiated, which results in a decrease of the fluorescence lifetime, e.g. ≅1 μs at 873 K (600 °C) for ruby.

A two-level model may be used to describe the temperature dependence of the fluorescence lifetimes due to the thermally activated repopulation between the ^2E (storage level) and $^4T_2$ (initial level) states at lower temperatures (300–600 K).

By taking account of the degeneracies of the $^4T_2$ and the ^2E states, a mathematical expression for the fluorescence lifetimes as a function of temperature can be obtained from the two-level model [1] as the following:

$$\tau = \tau_s \frac{1 + C_d\, e^{-\Delta E/k_B T}}{1 + (\tau_s/\tau_i)\, e^{-\Delta E/k_B T}} = \tau_s \frac{1 + 3\, e^{-\Delta E/k_B T}}{1 + \alpha\, e^{-\Delta E/k_B T}} \quad (2)$$

where τ is the fluorescence lifetime, τ_i and τ_s the lifetimes of the $^4T_2$ and ^2E states, C_d the ratio of the degeneracy of $^4T_2$ to that ^2E with a value of 3, ΔE the energy gap between the $^4T_2$ and ^2E states as defined in Eq. (1): $\Delta E\ (J) = 100hc\Delta E\ (cm^{-1})$, where $h = 6.625 \times 10^{-34}$ J s and $c = 2.998 \times 10^8$ m/s, $k_B = 1.38 \times 10^{-23}$ J/K.

The nonradiative transitions accelerate the decrease of the fluorescence lifetime with increasing temperature with an associated decrease in the fluorescence intensity. In this way, the single configurational model has been developed.

In a *low field crystal*, the lowest excited state is the $^4T_2$. The $^2E \rightarrow {}^2A_2$ transitions are one or two orders of magnitude weaker than the $^4T_2 \rightarrow {}^4A_2$ transitions, the latter being mainly determined for the fluorescence lifetimes. A single configurational coordinate model with only one excited state, as presented in Fig. 2, can describe the temperature dependence for fluorescence lifetimes. The excited and ground states involved are $^4T_2$ and $^4A_2$, respectively. These transitions occur via two processes: the first is the radiative transition initiated from I (the lowest energy point of the excited state), and the other is nonradiative, that is the thermal quenching of the Cr^{3+} ions which have been elevated to Q (the energy crossing of the excited and ground states) and which will rapidly lose energy to reach the bottom of the ground state through nonradiative relaxation, as is indicated in Fig. 2. The two processes are continuously competing with each other. The increasing temperature produces the more excited ions, which will be elevated to the energy level, Q (the nonradiative process will be the stronger). The nonradiative transitions are much faster, and as a result the $^4T_2 \rightarrow {}^4A_2$ transition rates increase with elevated temperature, and a decrease of fluorescence lifetimes with temperature is observed.

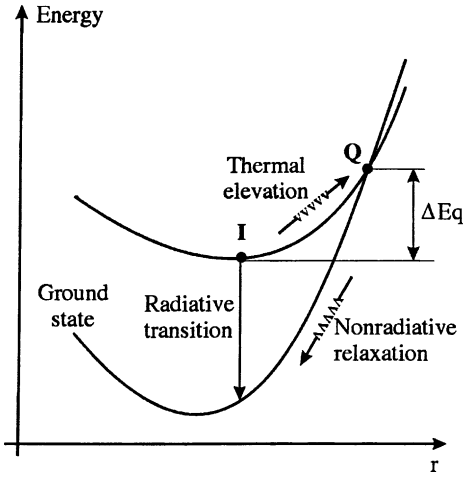

Fig. 2. The single configurational coordinate model for Cr^{3+} fluorescence in low field crystals.

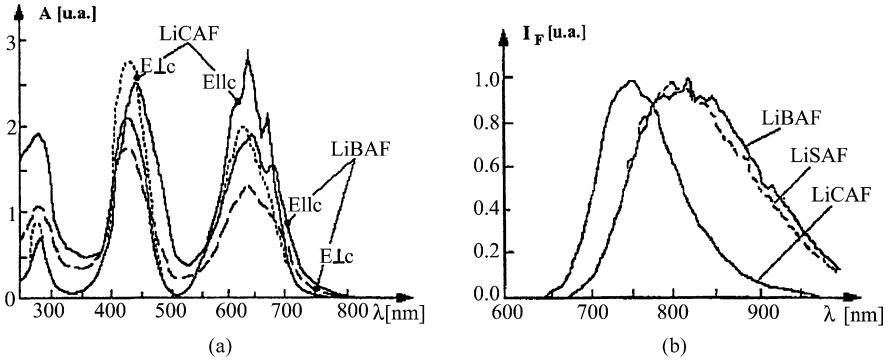

Fig. 3. (a) Absorption spectra for LiCAF and LiBAF crystals; (b) fluorescence emission for LiCAF, LiBAF and LiSAF crystals.

According to this model, the temperature dependence of the fluorescence lifetime of the Cr^{3+} may be given [1] by the equations:

$$\frac{1}{\tau} = \frac{1}{\tau_i} + \frac{1}{\tau_q} \times e^{-\Delta E_q/k_B T} \tag{3}$$

$$\tau = \tau_i \frac{1}{1 + \beta e^{-\Delta E_q/k_B T}} \tag{4}$$

where τ is the fluorescence lifetime, $\beta = \tau_i/\tau_q$ ($1/\tau_i$ is the intrinsic radiative rate at excited state and $1/\tau_q$ is the thermal quenching rate), ΔE_q the thermal activation needed to elevate the ions at the bottom of the excited state to the level crossing Q.

For example, in the case of LiSAF, a crystal very similar to the LiCAF of this study, the empirical values of these parameters are the following [1]: $\ln \beta = 18.89$, $\Delta E_q = 4557\ cm^{-1}$ and $\tau_i = 65.25\ \mu s$. An aspect of this study is the identification of these parameters for two Cr^{3+}:LiCAF crystals with 2 and 5% Cr^{3+} ions concentrations in this work.

Also, the temperature dependence of the fluorescence intensity is given [1] by a similar equation:

$$I = I_0 \frac{1}{1 + \beta e^{-\Delta E_q/k_B T}} \tag{5}$$

where I_0 is a constant determined by the scheme used.

The most important low field crystals, which can be used as the host for material Cr^{3+} dopant are LiCAF, LiBAF and LiSAF. For comparison, these fluorescent materials have absorption and fluorescent emission spectra as shown in Fig. 3 [1]. As may be expected, a close similarity in shape is seen, with some significant differences as well in the spectra presented [1,5]. For these crystals, the field strengths, *Dq/B* are in the order of 2.0.

3. Experimental method

A schematic of the optical fiber sensor is presented in Fig. 4. Two different LiCAF crystals, with Cr^{3+} concentrations of 2 and 5%, respectively were used in this study. These (shown as item 6 in the figure) were processed and polished, to give two identical and cylindrical crystals with 4 mm diameter and 2 mm thickness. These are reasonable sizes of crystals for handling and to achieve a satisfactory fluorescence level and thus they were incorporated in the probes.

The optical fibers (1 and 2) are fluoro-silica step index fibers of 1 m length and 600 μm core diameter. In the probe region (100 mm approximate length), the coating was striped and the active surface of the fibers was polished and finished to achieve a good contact with the crystals. The ceramic fixtures (4 and 5) were used for thermal stability and the thermo-constrictive muff (3) for impact protection of the probe. The ensemble was held together with FORTAFIX adhesive (chosen because of its resistance to high temperatures). Further, the crystals were immobilized with a bead of FORTAFIX (7), after finishing, washing and drying. The others ends of the optical fibers were mounted the SMA connectors with the usual termination procedure.

The optoelectronic system used for this application is relatively simple and has the set-up presented as a schematic in Fig. 5.

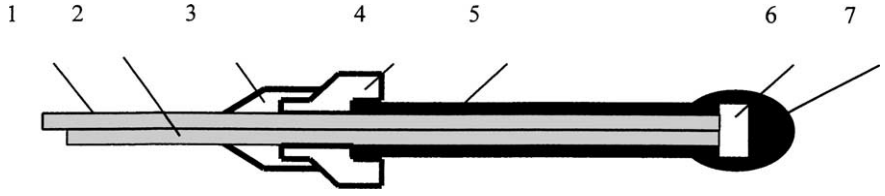

Fig. 4. Optical fiber sensor for temperature measurement: 1, 2, optical fibers carrying light in and out; 3, 4, mechanical fixtures of the probe; 5, outer ceramic sheath; 6, crystal; 7, adhesive coating.

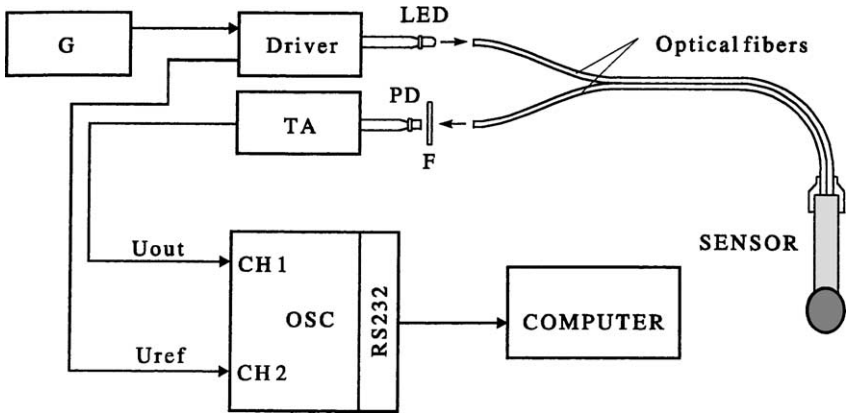

Fig. 5. The optoelectronic arrangement of the measurement system.

This system contains (item numbers from Fig. 1):

1. sensor: optical fiber sensor (the probe);
2. F: ''high pass'' optical filter (RGB695)—for filtering of the fluorescence light emission;
3. LED: blue ultrabright light emission diode ($\lambda_p = 450$ nm, spectral width about 20 nm, $I_v = 1000$ mcd) with the emission spectrum in a strong absorption region of the LiCAF absorption spectrum;
4. PD: photodiode, type BPX65;
5. driver: electronic driver for the LED current excitation ILED, driven by a frequency generator, G;
6. G: stable frequency generator;
7. TA: transimpedance amplifier using an operational amplifier OPA111BM (low noise, Bi-FET);
8. OSC: digital oscilloscope with RS232 interface (HP54600A) CH1, CH2 input parts;
9. computer.

Further, the measurement system includes an electric oven with a temperature control which was used with a Pt 100 RTD thermometer probe and a high accuracy multimeter (HP5400A) for ease of temperature calibration of the system described. The optical probe performance data were obtained for stable values over a range of temperatures. Practically, the wave generator (G) gives a voltage with a sinusoidal variation, and the electronic driver (driver) converts this voltage into an excitation current for the LED ($\cong$40 mA_{pp}). This current, I_{LED}, can be measured indirectly with a standard resistance ($R_s = 10\,\Omega$) and the sensor response is obtained at the photodiode (PD). This photocurrent is converted in an output voltage, U_{out}, with the transimpedance amplifier (TA). The I_{LED} and U_{out} signals are obtained with the acquisition system (OSCiloscope-computer), the result being a data file (''asc'' file) which is processed by MATLAB software (Fig. 6). Because the U_{out} signal is affected by the inevitable noise present, a Butterworth digital filter ($n = 4$ poles, $f_{cut} = 2$ kHz) is used for noise rejection (the frequency magnitude characteristic of this filter is presented in Fig. 6c).

The filtering process is applied to the two signals. the reason being that the result required of the measurement itself is the time delay between these signals and the filtering process will have a negligible effect on it. The result is presented in Fig. 6b and the spectral power of the U_{out}, before and after filtering process, is shown in Fig. 6d. The MATLAB program gives the following quantities:

- Δt_m—the delay time between the reference sine signal (light excitation) and response signal: it is obtained after the filtering operation (Fig. 6b), where this delay time must be corrected because the transimpedance amplifier introduces an intrinsic delay time, Δt^* (this delay time is obtained by empirical observation for $f = 2$ kHz, $\Delta t^* = 23$ μs);
- Δt_{cm}—the corrected delay time is the real delay time, which can be used for the fluorescence lifetime calculation:

$$\Delta t_{cm} = \Delta t_m - \Delta t^* \tag{6}$$

- τ_{cm}—the fluorescence lifetime for the crystals is obtained from Δt_{cm}:

$$\tau_{cm} = \frac{tg(2\pi f \Delta t_{cm})}{2\pi f} \tag{7}$$

4. Probe calibration results

The measured data for the two samples of LiCAF (Cr^{3+}: 2%) and LiCAF (Cr^{3+}: 5%) are presented in the Tables 1 and 2.

Using the obtained data, τ_{cm}, the mathematical model (Eq. (4)) and the mathematical regression software (''Data Fit''), the parameters of the model used are obtained, these being τ_i, β and ΔE_q (cm^{-1}, Table 3). Following that, using Eq. (4) and these parameters, the fluorescence lifetime, τ was calculated (sample data for which are presented in the tables).

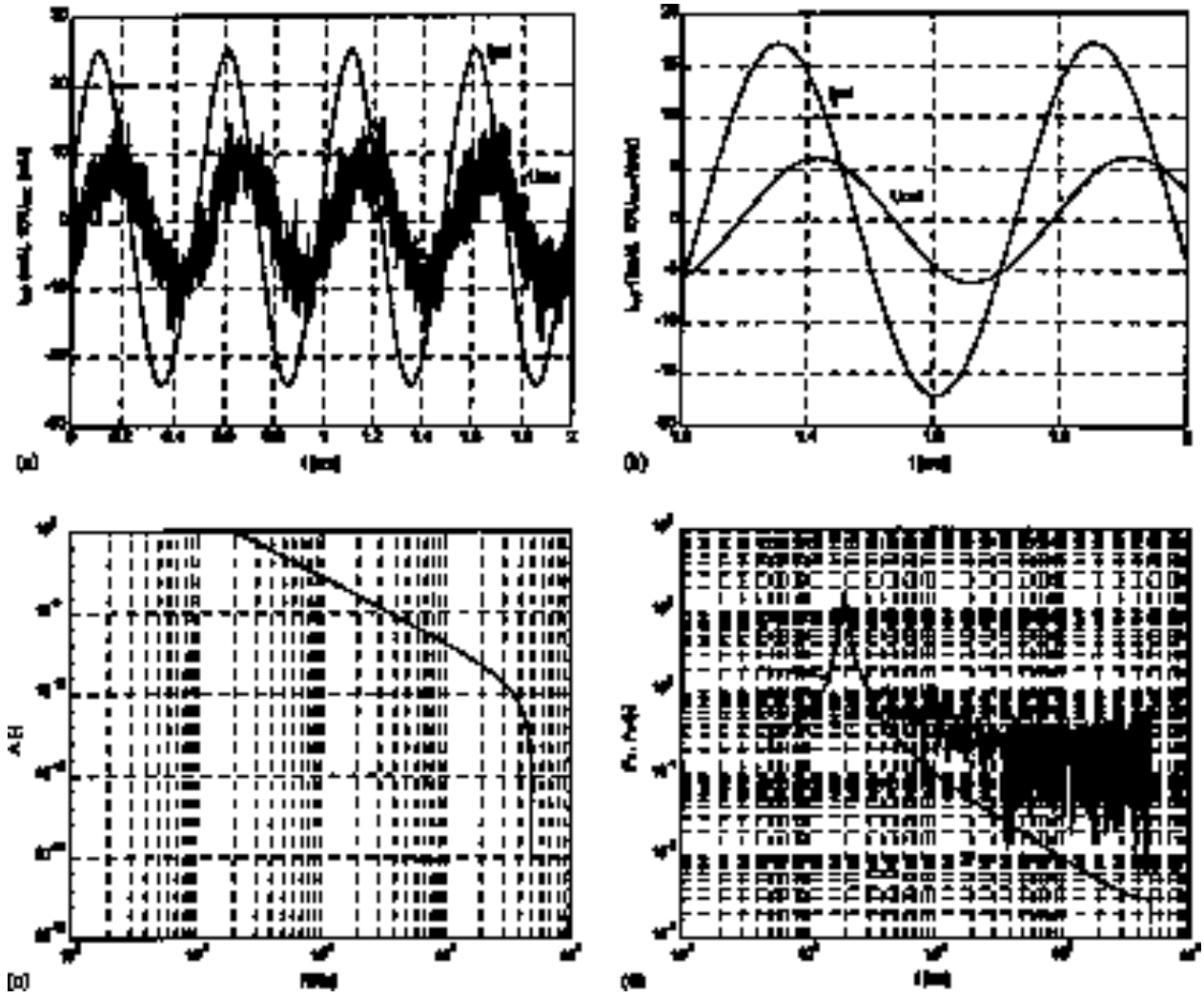

Fig. 6. (a) Typical I_{LED} and U_{out} signals obtained from the system; (b) I_{LED} and U_{out} signals after the digital filtering; (c) the frequency–amplitude characteristic of the digital Butterworth filter ($n = 4$ poles, $f_{out} = 2$ kHz); (d) the spectral power for the U_{out} voltage before and after the processing filter.

Table 1
Experimental data for LiCAF (Cr^{3+}: 2%)

θ (°C)	22.28	66.41	101.59	141.24	168.24	203.68	231.33	253.49
T (K)	295.43	339.56	374.74	414.39	441.39	476.83	504.48	526.64
Δt_m (μs)	108	108	106	106	103	85	58	30
Δt_{cm} (μs)	85	85	83	83	80	62	35	7
τ_{cm} (μs)	144.75	144.75	136.51	136.51	125.39	78.58	37.45	7.02
τ (μs)	140.92	140.91	140.81	138.49	127.57	78.14	33.31	14.28

Table 2
Experimental data for LiCAF (Cr^{3+}: 5%)

θ (°C)	30.33	58.33	102.49	177.76	214.51	242.55	266.37
T (K)	303.48	331.48	375.64	450.91	487.66	515.70	539.52
Δt_m (μs)	111	107.3	107.6	102	85.5	49.75	37
Δt_{cm} (μs)	88	84.3	84.6	79	62.5	26.75	14
τ_{cm} (μs)	158.6	141.78	143.04	121.97	79.58	27.81	14.15
τ (μs)	146.97	146.97	146.81	127.35	73.62	32.94	14.69

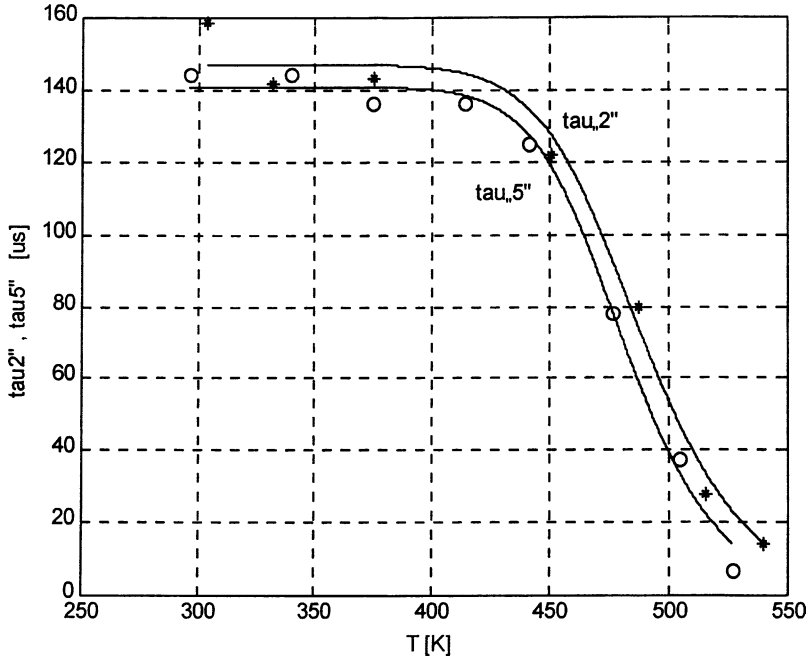

Fig. 7. Temperature dependences of the fluorescence lifetimes of LiCAF crystals.

Table 3
Crystal parameters for LiCAF—2 and 5%

Concentration of Cr^{3+} (%)	τ_i (μs)	ln(β)	ΔE (cm^{-1})
2	140.92	25.17	8413.92
5	146.97	22.90	7762.70

Fig. 7 presents graphically the characteristic of the measurement system for both crystals. The points describe the values obtained by measuring τ_{cm} and the curves were obtained by using the regression method for τ where the curves are:

- tau2: for LiCAF crystal with Cr^{3+}—2% concentration;
- tau5: for LiCAF crystal with Cr^{3+}—5% concentration.

5. Discussion

This work, and the results obtained, have shown the potential and capability of a fiber optic thermometer probe based on LiCAF [6], following studies carried out with the two samples of different dopant concentration discussed. The work shows that the Cr^{3+} ion concentration in the LiCAF host crystal does not have a very important influence on the calibration and a higher species density gives a stronger absorption and fluorescence signal. For example, in the case of ruby, the fluorescence lifetime decreases significantly with the increase of the Cr^{3+} ion concentration [1,7], but for the LiCAF, this concentration influence is negligible [6]. It can be observed that the two curves in Fig. 7 are similar in shape and slightly offset one from the other and the parameters of the mathematical model resulting from the work are broadly similar. Practically, the measurement system has same sensitivity for both crystals (the two curves have the same shape) of approximately 0.625 μs/°C over the 400–550 K region.

The results show the same characteristic feature as was seen for a LiSAF probe investigated earlier by some of the authors [6]. This material also has a region of relatively stable lifetime with temperature, followed by a rapid reduction in lifetime as the temperature increases, but with the region of the highest sensitivity (in the LiCAF case this region is between 425 and 550 K) shifted to higher temperature. The LiSAF probe [6] was optimized as a result for the biomedical measurement region (300–330 K) but the LiCAF probe is of little value over this temperature region.

The optimum sensitivity temperature domain is beyond 150 °C, covering the region from 425 to 550 K. This corresponds well with the boiling temperatures of certain oils and such a probe would be well suited to this type of monitoring application. An application which has been brought to the authors' attention is monitoring heating effects in oil-filled transformers. In particular, the optical nature of the measurement is well suited to use with inflammable materials of this type as no currents are present at the probe. In particular, transformer overheating can be highly dangerous if the oils involved become volatile and in some cases potentially explosive. Such a probe could be built into a transformer during winding of the coils or retrofitted.

The decrease of the peak to peak amplitude for U_{out} (fluorescence intensity), following Eq. (5) sets an effective limit on the upper temperature, of use of the probe in the same way as occurs with ruby, with a rapidly by reducing

lifetime and a dissemination of the fluorescence intensity emitted. One solution to give an extended range is a more sensitive detection system, which could be designed, but this will only give a limited improvement. Other species, e.g. neodymium or erbium in YAG or glass offer better performance at these higher temperatures [1]. The sinusoidal wave excitation method allowed the obtaining of the best signal/noise ratio, thereby giving a good resolution, typically ± 2 K over the sensitive region, this figure arising from typical uncertainties in measurements averaged over a few seconds period.

Acknowledgements

The authors are pleased to acknowledge the support of EPSRC via the INTErSECT Faraday Partnership for the provision of resources used in this work.

References

[1] Z.Y. Zhang, K.TV. Grattan, Fiber Optic Fluorescence Thermometry, Chapman & Hall, London, 1995.
[2] Z.Y. Zhang, K.T.V. Grattan, A.W. Palmer, B.T. Meggitt, Thulium-doped intrinsic fiber optic sensor for high temperature measurements (>1100 °C), Rev. Sci. Instruments 69 (1998) 3210–3214.
[3] Z.Y. Zhang, K.T.V. Grattan, A.W. Palmer, Fiber optic thermometry based on fluorescence lifetimes of Cr^{+3}-doped materials, Proc. SPIE 2121 (1993) 476–482.
[4] W.H. Fonger, C.W. Struck, Temperature dependences of Cr^{3+} radiative and nonradiative transitions in ruby and emerald, Phys. Rev. B 11 (9) (1995) 3251–3260.
[5] M. Stalder, B.H.T. Chai, M. Bass, Crystal Growth and Spectroscopy of Cr:$LiBaAlF_6$, in: Proceedings of the Advanced Solid State Lasers Topical Meeting, 18–20 March, Paper ME4, Head Island, SC, 1991.
[6] Z.Y. Zhang, K.T.V. Grattan, A.W. Palmer, Cr:LiSAF fluorescence lifetime based fiber optic thermometer and its application in chemical RF heat treatment, in: Proceedings of the International Conference on Advances in Fluorescence Using Technology, Biomedical Optics'93, Los Angeles, 1993.
[7] G.F. Imbusch, Inorganic luminescence, in: M.D. Lumb (Ed.), Luminescence Spectroscopy, Academic Press, New York, 1978, p. 78.

Biography

K.T.V. Grattan was born in Co. Armagh, Northern Ireland on 9 December 1953. He received his Bachelors degree in physics (with first class honors) from The Queen's University, Belfast in 1974 and completed his PhD studies in 1978, graduating from the same university. In the same year, he became a post-doctoral research assistant at Imperial College, London. His research during that period was on laser systems for photophysical systems investigations. His work in the field continued with research using ultraviolet and vacuum ultraviolet lasers for photolytic laser fusion driver systems and studies on the photophysics of atomic and molecular systems.

He joined City University, London in 1983 after 5 years at Imperial College, undertaking research in novel optical instrumentation, especially in fiber optic sensor development for physical and chemical sensing. The work has led to several fields including luminescence-based thermometry, Bragg grating-based strain sensor systems, white light interferometry, optical system modeling and design and optical sensors for water quality monitoring. The work has been extensively published in the major journals and at international conferences in the field, where regularly he has been an invited speaker, and over 500 papers have been authored to date. He was awarded the degree of Doctor of Science by City University in 1992.

Professor Grattan is currently Associate Dean of Engineering at City University, London having from 1991 to 2001 been Head of the then Electrical, Electronic and Information Engineering Department. He was Chairman of the Applied Optics Division of the UK Institute of Physics and President of the Institute of Measurement and Control in 2000.